Efficiency Enhancement in Polymer Solar Cells With a Polar Small Molecule Both at Interface and in the Bulk Heterojunction Layer

Zhengguo Xiao, Qingfeng Dong, Qi Wang, Wenjing Tian, Hui Huang, and Jinsong Huang

Abstract—The polar molecules, including ferroelectric materials with large dipole moments, have been applied as interfacial layers to increase the efficiency of organic solar cells by increasing the bounded charge separation, tuning the energy levels, etc. Here, we report a small polar molecule 2-cyano-3-(4-(diphenylamino) phenyl)acrylic acid (TPACA) that can be either blended in the active layer or at the polymer/electrode interface to increase the efficiency of organic solar cell devices after poling. It is found that the built-in potential of the device is increased by 0.2 V after poling under negative bias. Blending TPACA into the active layer has shown to be a universal method to increase the efficiency of polymer solar cells. The efficiency is increased by 30–90% for all the polymer:fullerene systems tested, with the highest efficiency reaching 7.83% for the poly[4,8-bis-(2-ethyl-hexyl-thiophene-5-yl)-benzo[1,2-b:4,5-b']dithiophene-2,6-diyl]-alt-[2-(2′-ethyl-hexanoyl)-thieno[3,4-b]thiophen-4,6-diyl]: [6,6]-phenyl-C_{71}-butyric acid methyl ester (PBDTTT-CT:PC_{70}BM) system.

Index Terms—Interfacial layer, organic solar cell, polar molecules.

I. INTRODUCTION

OVER the past few decades, organic solar cells (OSCs) have attracted tremendous attention due to their advantages of low-cost manufacturing and flexibility [1], [2]. With great efforts from the community, the power conversion efficiency (PCE) of OSCs has exceeded 10% for a single-junction cells and 12% for tandem cells [3]–[6]. Interfacial layers play important but different functions in improving OSC performance. Dielectric materials such as lithium fluoride (LiF) and caesium carbonate (Cs_2CO_3), metal oxides such as zinc oxide (ZnO) and titanium oxide (TiO_2), and n-type organic/polymer conjugated materials are employed as electron transporting

and/or hole blocking layers [7]–[10]. Polar materials is a very promising interfacial layers and have been broadly applied in OSCs to increase its efficiency [11], [12]. Organic molecules with strong dipole moments have been employed to increase the internal electric field of the OSCs to achieve a high open-circuit voltage (V_{OC}). For example, an aligned surface-segregated monolayer of fluorinated compounds was inserted at the donor/acceptor (D/A) interface, which resulted in the change of the V_{OC} from 0.3 to 0.95 V [11], [13]. Chen *et al.* applied a self-assembled conjugated polyelectroyte-ionic liquid crystal complex as an interlayer to tune the work function of the electrodes to increase device performance via rapid liquid crystal-induced dipole orientation [14]. Recently, we reported a new category of air stable material, ferroelectric polymer poly(vinylideneuoride-tri uoroethylene) (P(VDF-TrFE)), as interfacial layer which has large density of field switchable dipoles [15]–[18]. This ferroelectric material can be inserted at the polymer/electrode interface to tune the work function of the metal electrode, which results in higher short-circuit current (J_{SC}) and fill factor (FF) due to the increased internal electric field after poling. P(VDF-TrFE) can also be inserted at the donor/acceptor interface to tune their energy offset, which results in higher V_{OC}. The V_{OC} of the poly(3-hexylthiophene) (P3HT): [6,6]-phenyl-C_{61}-butyric acid methyl ester (PC_{60}BM) system increased to 0.68 V due to the smaller lowest unoccupied molecular orbital (HOMO) energy offset between P3HT and PC_{60}BM after poling [16], [17].

In this contribution, we report the integration of a polar small molecule 2-cyano-3-(4-(diphenylamino)phenyl)acrylic acid (TPACA) [see Fig. 1(a)] into the device to improve the V_{OC} and PCE of OSCs by tuning the internal electric field. Organic dyes that contain donors with triphenylamine or its derivatives and cyano-acrylic acid acceptors bridged by a methine fragment have been used as efficient sensitizers in dye-sensitized solar cells [19], [20] because the molecules are noncoplanar and chemical stable. In addition, these organic dyes have strong dipole moments due to their D-π-A structures. TPACA can be inserted at the polymer/electrode interface or easily blended in the active layer to increase the device efficiency. The efficiency of the OSC device has been increased by 30–90% for all the systems tested, including P3HT, poly[N-9′-hepta-decanyl-2,7-carbazole-alt-5,5-(4′,7′-di-2-thienyl-2′,1′,3′-enzothiadiazole)] (PCDTBT) and poly[4,8-bis-(2-ethyl-hexyl-thiophene-5-yl)-benzo[1,2-b:4,5-b']dithiophene-2,6-diyl]-alt-[2-(2′-ethyl-hexanoyl)-thieno[3,4-b]thiophen-4,6-diyl] (PBDTTT-CT), with the highest efficiency reached 7.83% for the PBDTTT-CT: [6,6]-phenyl-C_{71}-butyric acid methyl ester (PC_{70}BM) system.

Z. Xiao, Q. Dong, Q. Wang, and J. Huang are with the Department of Mechanical and Materials Engineering, Nebraska Center for Materials and Nanoscience, University of Nebraska, Lincoln, NE 68588-0656 USA (e-mail: zg.xiao1@gmail.com; qingfeng.dong@gmail.com; qiwangunl@gmail.com; jhuang2@unl.edu).

W. Tian is with the State Key Laboratory of Supramolecular Structure and Materials, Jilin University, Changchun 130012 China (e-mail: wjtian@jlu.edu.cn).

H. Huang is with the College of Materials Science and Opto-electronic Technology, University of Chinese Academy of Sciences, Beijing 100049, China (e-mail: huihuang@ucas.ac.cn).

Color versions of one or more of the figures in this paper are available online at http://ieeexplore.ieee.org.

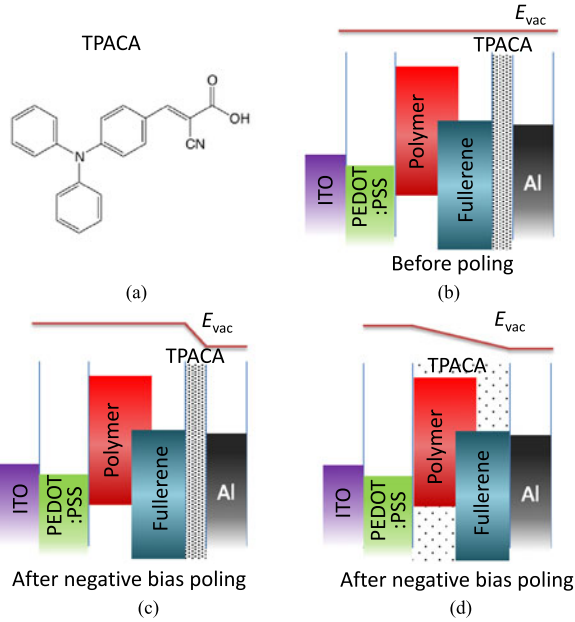Digital Object Identifier 10.1109/JPHOTOV.2015.2455672

Fig. 1. (a) Molecular structure of TPACA. Energy diagram of the device (b) before poling and (c) after negative bias poling with TPACA as the cathode interfacial layer. (d) Energy diagram of the device after negative bias poling with TPACA blend in the active layer.

II. MATERIALS AND METHODS

A. Materials

Poly(3,4-ethylenedioxythiophene):Polystyrene sulfonate (PEDOT:PSS) was purchased from H.C. Starck. RR-P3HT and $PC_{60}BM$ were purchased from Rieke Metals and nano-C, respectively. PBDTTT-CT was purchased from Solarmer Energy, Inc. (molecular weight: around 29 KDa); PCDTBT was provided by Konarka Technologies (molecular weight: approximately 100 K). They were used as received.

B. Methods

1) Device Fabrication: PEDOT:PSS (Baytron-P 4083) was spin coated on clean ITO substrate at a speed of 3000 r/min. The film was then annealed at 130 °C for 30 min. Different solutions of polymer:fullerene-derivative were then spin coated on top of dry PEDOT:PSS film in the N_2 filled glove box (polymers and fullerene-derivatives concentration. For the device with TPACA as interfacial layer, the TPACA (dissolved in methanol, 0.5% wt) was spun on top of the dried polymer:fullerene film at 3000 rpm for 30 s. For the device with TPACA blended in the active layer, the TPACA was added in the polymer:fullerene solution with different weight ratio. Afterwards, the device was finished by thermal evaporating aluminum (100 nm). The spin coating parameters of the polymer:fullerene film and the TPACA weight ratio are described in Table I.

2) Device Measurement: All devices were measured under simulated AM 1.5G irradiation, (100 mW/cm^{-2}) with a xenon-lamp-based solar simulator. The poling of the device was conducted at room temperature, the negative and positive bias poling pulse is −13 V and +3 V for 10 s, respectively.

The dependence of the free-charge generation ratio with different applied bias was measured by the time delayed collection field (TDCF) method. The laser intensity of the N_2 laser, with a shot-to-shot energy deviation of <3%, was attenuated by neutral density filters so that the photocurrent pulse height generated was comparable to the J_{SC}. An upgraded Keithley semiconductor parameter analyzer (4200-SCS) with two synchronized voltage output channels was used to trigger the nitrogen laser and provide charge collection bias, respectively. The rising time of the trigger pulse and the electrical bias pulse was 10 ns. The nitrogen laser provides a simultaneous TTL pulse output with a full width at half maximum (FWHM) of 1 ns during the laser pulse output, enabling an accurate identification of the delay time between the laser pulse and charge extraction pulse. A digital oscilloscope with a bandwidth of 500 MHz was used to record the voltage pulse over a 50-Ω resistance, which was connected in series with the device.

The charge extraction time measurement setup is the same as that used for free-charge generation ratio measurement. The only difference is that the bias applied on the device was kept the same during the laser pulse illumination, while, for the charge generation ratio measurement, the bias of on the device was switched to −4 V after a delay of 500 ns after the laser pulse illumination.

The capacitance of the device was measured in the dark using *LCR* meter (Agilent, E4980A) at 100 kHz.

III. RESULTS AND DISCUSSION

A. 2-Cyano-3-(4-(Diphenylamino) Phenyl)Acrylic Acid as Cathode Interfacial Layer

In our experiments, P3HT- and $PC_{60}BM$-based bulk heterojunction solar cells were initially used as the standard cell to evaluate the function of the dipole molecules since it is a well-established material system [15], [21]. A regular device structure of ITO/PEDOT:PSS/polymer:fullerene/Al was employed. One advantage of this structure is the absence of low work function metals like calcium (Ca), which can increase the stability of the devices. TPACA, dissolved in ethanol, was spun on top of the dry P3HT:$PC_{60}BM$ layer to form a cathode interfacial layer. Fig. 1(b) and (c) shows the energy diagram of the pristine device and after poling with TPACA at the cathode interface. After negative bias poling, the dipoles of the TPACA are aligned, which can increase the work function of the Al cathode. The current density–voltage (*J–V*) curves are shown in Fig. 2(a). Without poling, the J_{SC}, V_{OC}, FF, and PCE of the solar cell device were 7.90 mA/cm^2, 0.43 V, 56.4%, and 1.91%, respectively. After poling under −13 V for around 10 s, the V_{OC} increased from 0.43 to 0.59 V. In addition, an increase in J_{SC} of 0.60 mA/cm^2 and an enhancement of FF from 56.4% to 70.4% were also observed after poling the TPACA film by a negative bias. Thus, the PCE was increased from 1.91% to 3.53%. This indicates that, after negative bias poling, TPACA molecules will be aligned to form a dipole pointing from Al to active layer, same as the direction of the built-in electric field pointing from Al to ITO, resulting in an increase of the built-in electric field.

TABLE I
DIFFERENT POLYMER: FULLERENE-DERIVATIVE BLEND FILMS FABRICATION DETAILS (DIO(1,8-DIIODOOCTANE))

| Materials	PBDTTT-CT:PC_{70}BM	PCDTBT:PC_{70}BM	P3HT:PC_{60}BM
Polymer:fullerene weight ratio (polymer concentration)	1:1.5	1:4 (4 mg/ml)	1:1 (17.5 mg/ml)
Working solvent	DCB	DCB:CB (3:1 V/V)	DCB
TPACA weight ratio	100:150:1	40:160:1	200:200:1
Spin coating parameter	900 r/min for 60 s	2400 r/min for 14 s	800 r/min for 20 s
Annealing condition	No annealing	No annealing	150 °C for 10 min
Film thickness	~105 nm	~80 nm	~150 nm
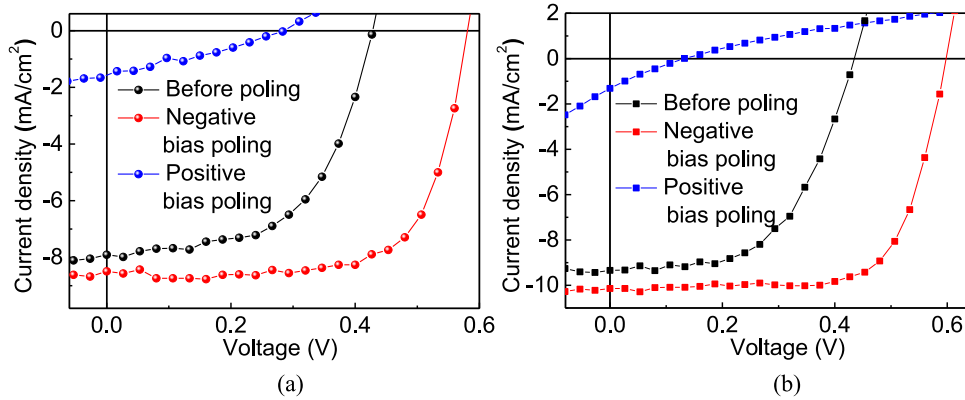
Fig. 2. (a) Photocurrent of the P3HT:PC_{60}BM device before and after negative bias poling with TPACA as cathode interfacial layer. (b) Photocurrent of the P3HT:PC_{60}BM device before and after poling with TPACA blended in the active layer.

B. 2-Cyano-3-(4-(Diphenylamino) Phenyl)Acrylic Acid Blended in the Active Layer

One unique property of small polar molecule TPACA over ferroelectric materials is that it can be dissolved in processing solvent like DCB so that it can be simply blended in DCB with polymers and fullerenes. Here, the TPACA was added in the P3HT:PC_{60}BM blend solution before spin coating. It is noted that the weight ratio of the TPACA in the P3HT:PC_{60}BM bulk heterojunction film is only 0.25% (see Table I). More TPACA would ruin the film morphology and decrease the device performance. In this case, the TPACA is expected to be in the bulk active layer rather than at the interface between active layer and electrode. After negative bias poling, the dipoles of TPACA in the bulk can also be aligned, which result in increasing of the work function of the cathode as shown in Fig. 1(d). As shown in Fig. 2(b), before poling, the J_{SC}, V_{OC}, FF, and PCE of the device are 9.34 mA/cm^2, 0.43 V, 55.8%, and 2.22%, respectively, which are comparable with the device without TPACA blended in the active layer. After poling at −13 V for around 10 s, the efficiency increased to 4.32% with a J_{SC} of 10.2 mA/cm^2, a V_{OC} of 0.60 V, and an FF of 70.6%. To verify that the orientation of the dipole moment of the polar molecules is critical for the device performance, the P3HT:PC_{60}BM-based solar cell with TPACA in the bulk was poled at +3 V to switch the dipole direction. As shown in Fig. 3(b), after forward bias poling, the efficiency dramatically decreased to 0.04% with a J_{SC} of 1.31 mA/cm^2, a V_{OC} of 0.13 V, and an FF of 21.0%. Here, a lower poling voltage was used to avoid the burning of the device by the large injection current. This indicates that the forward bias poling led to unfavorable dipole moment pointing from indium tin oxide (ITO)

toward Al, which dramatically reduced the built-in electric field in the active layer.

Blending the P3HT:PC_{60}BM and TPACA in one-step spin coating can be simpler comparing to fabricating double layer of P3HT:PC_{60}BM and TPACA films in two steps. One may argue that TPACA may self-assemble to form a thin layer on top of P3HT:PC_{60}BM during the slow dry process after spin-coating the blending film of P3HT:PC_{60}BM:TPACA. For clarification, we measured the contact angle of the P3HT:PC_{60}BM films with and without TPACA blended in the active layer. TPACA is more hydrophilic than the P3HT:PC_{60}BM film so that the contact angle of the film is expected to be smaller if the TPACA molecules are self-assembled at the top surface after thermal annealing. However, as shown in Fig. 3(a) and (b), the contact angles of both films with and without TPACA are the same at 91°, which indicate that the TPACA molecules are blended in the active layer. In addition, two control experiments were carried out. First, after spin coating of TPACA film on top of P3HT:PC_{60}BM film where TPACA worked as interfacial layer, methanol was used to wash the film. Second, methanol was employed to wash the bulk film where TPACA was blended in the bulk. As shown in Fig. 3(e) and (f), there is no poling effect for the devices with TPACA interfacial layer after methanol wash, which indicates that methanol can wash off the TPACA on top of the blend film. However, the performance of solar cell devices with TPACA blended in the bulk P3HT:PC_{60}BM films still has an obvious enhancement after the poling. This indicates that after spin coating the P3HT:PC_{60}BM:TPACA mixed solution, the TPACA stays inside of the bulk film P3HT:PC_{60}BM after the film preparation.
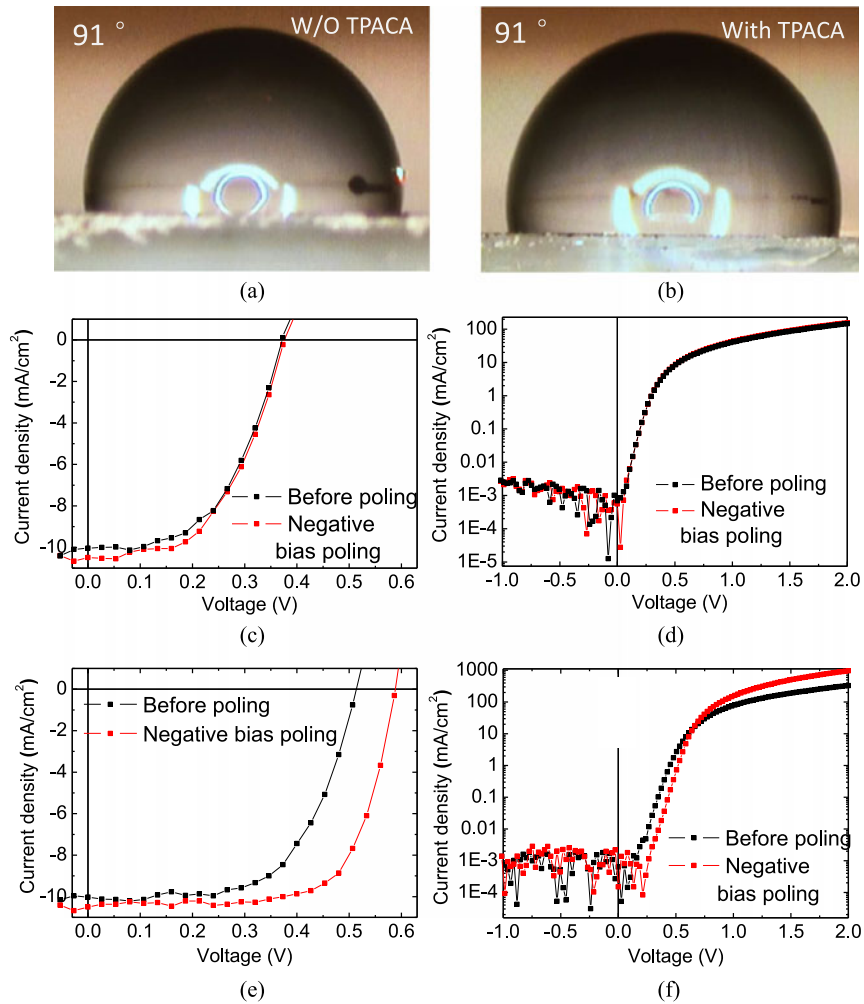
Fig. 3. Contact angle measurement of the PHT:PC$_{60}$BM film (a) without and (b) with TPACA blended in the active layer. (c) Photocurrent and (d) dark current of the device before and after negative bias poling after methanol washing with TPACA as interfacial layer. (e) Photocurrent and (f) dark current of the device before and after negative bias poling after methanol washing with TPACA blended in the P3HT:PC$_{60}$BM active layer.

C. Origin of the Efficiency Enhancement

It is noted that the performance enhancement using small polar molecules is different from the reported system where doping P3HT:PC$_{60}$BM with ferroelectric dipoles resulted in increase of J_{SC} and FF and no change of V_{OC} after negative bias poling [22]. In our case, the main increase of the PCE is due to the larger V_{OC} after poling. The increased V_{OC} can be reflected by the reduced saturated dark current of the devices and the built-in potential measured by the capacitance. As shown in Fig. 4(a), the negative bias poling reduces the reverse saturated dark current by two orders of magnitude. This can be understood from the general expression for V_{OC} in OPV devices:

$$V_{OC} = \frac{nkT}{q} \ln\left(\frac{J_{SC}}{J_0} + 1\right) \qquad (1)$$

where k is the Boltzmann constant, T is the temperature, q is the elemental electron charge, J_{SC} is the photocurrent density due to exciton dissociation, J_0 is the saturated dark current density, and n is the diode ideal factor.

The built-in potential of the device was found out by the capacitance versus voltage measurement. Fig. 4(b) shows built-in

potential of the P3HT:PC$_{60}$BM:TPACA device before and after negative bias poling, measured by fitting the $1/C^2$ versus voltage. The device was measured at 100 KHz in the dark using *LCR* meter [23]. The built-in potential was increased from 0.47 V before poling to 0.66 V after negative bias poling, which is correlated with the V_{OC} of the devices under different poling conditions. The slightly increased J_{SC} and FF after negative bias poling the device can be explained by the reduced charge recombination due to the increased built-in electric field.

In order to examine the influence of increased built-in electric field on the charge generation and transporting property of the device, both charge generation efficiency and charge extraction time were measured on the P3HT:PC$_{60}$BM-based device with TPACA blended in the active layer. It is believed that the primary photoexcitations in organic semiconductors are strongly bound Frenkel excitons, while only free charges contribute to photocurrent. Two models have been proposed to explain the fundamental processes resulting in the formation of extractable free charge carriers [24], [25]. In the first model, the separation of the excitons forms Coulombically bound electron–hole pairs (polaron pairs, PPs) at the donor–acceptor heterojunction.
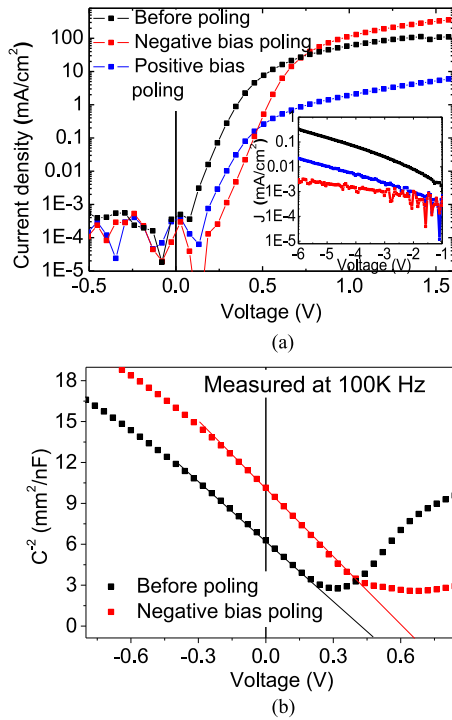
Fig. 4.   (a) Dark current of the device with TPACA blended in the active layer. The inset is the dark current of the device under negative bias. (b) Built-in potential of the P3HT:PC$_{60}$BM device measured by fitting the $1/C^2$ versus voltage curve.
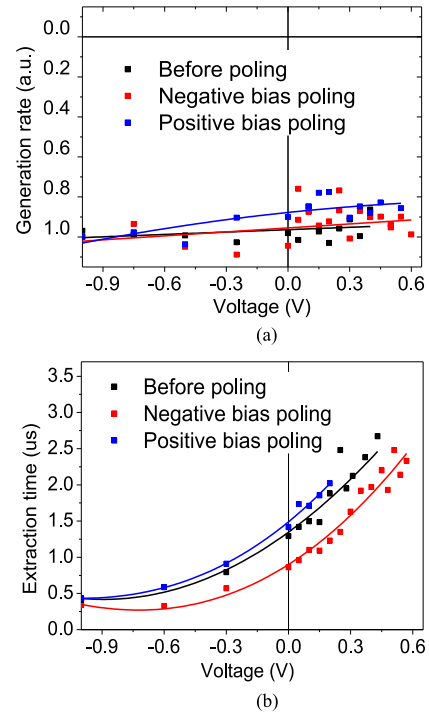

Fig. 5.   (a) Charge generation rate measured by time delayed collection field. The charge generation efficiencies were measured under different bias from -4 V to open-circuit voltage and were normalized by the internal quantum efficiency at -4 V. (b) Charge extraction time of the device before and after poling.

In this case, the carrier generation yield can be enhanced in the presence of an electric field, while a small fraction of PPs can separate into free carriers by diffusion. In the second model, exciton dissociation directly yields free carriers, indicating that the electric field should not influence the formation of extractable carriers [25]. To probe the photogeneration of the P3HT:PC$_{60}$BM:TPACA blended film-based solar cells, TDCF experiments [26], [27] were employed to study the relationship between free charge generation yield and the bias applied on the device. In our system, different bias (from -4 to $+0.6$ V) was applied at the devices during the excitation and prior to the application of charge collection bias of -4 V. The rising time of the trigger pulse and the electrical bias pulse was 10 ns. After a delay time of 500 ns which is much less than the charge carrier lifetime in the P3HT:PC$_{60}$BM system [28], a collection bias of -4 V was employed to sweep the carriers through the organic layer and extract them at the electrodes. As shown in Fig. 5(a), the charge generation yield is bias independent in the P3HT:PC$_{60}$BM system, which agrees with previous study [29], and the charge generation yield is the same for the device under different poling conditions. This means that the increased internal electric field after negative bias poling did not increase the charge generation. On the other side, the charge extraction time shown in Fig. 5(b) was decreased at the same voltage after negative bias poling, which indicates that the internal electrical field can facilitate the charge extraction after negative bias poling. For the charge extraction time measurement, the bias applied on the device was kept the same after the laser pulse illumination.

D. Universal Application of the 2-Cyano-3-(4-(Diphenylamino) Phenyl)Acrylic Acid in Other Polymer:Fullerene Systems

It is exciting that blending TPACA in the bulk active layer is a general method to increase the OSC device efficiency. Here, two low-bandgap polymers PCDTBT and PBDTTT-CT were employed to fabricate the devices with a regular structure of ITO/PEDOT:PSS/polymer:PC$_{70}$BM:TPACA/Al. The device fabrication details including the TPACA weight ratio in the bulk active layer are described in the experiment details section. The J–V curves are shown in Fig. 6. For PCDTBT polymer, the efficiency of the solar cells increased from 4.45% to 5.79% with enhanced V_{OC} and FF, but a same J_{SC} after negative bias poling. The efficiency is higher than the reported efficiency (5.4%) of the PCDTBT-based solar cells with a regular structure of ITO/PEDOT:PSS/PCDTBT:PC$_{70}$BM/Ca/Al in our system with higher V_{OC} and FF [17]. For the PBDTTT-CT:PC$_{70}$BM system, after negative bias poling, the V_{OC} and FF were enhanced, and J_{SC} was improved slightly, resulting in a significantly improved efficiency of 7.83%, which is also much higher than our previously reported efficiency (7.0%) for this polymer with the device structure of ITO/PEDOT:PSS/PBDTTT-CT:PC$_{70}$BM/Ca/Al [30].

IV. CONCLUSION

In conclusion, a polar molecule, TPACA, was employed to tune the built-in electric field of the OSCs to improve their device performances. TPACA can either be inserted at the cathode interface as an interfacial layer, or blended in the bulk active layer.
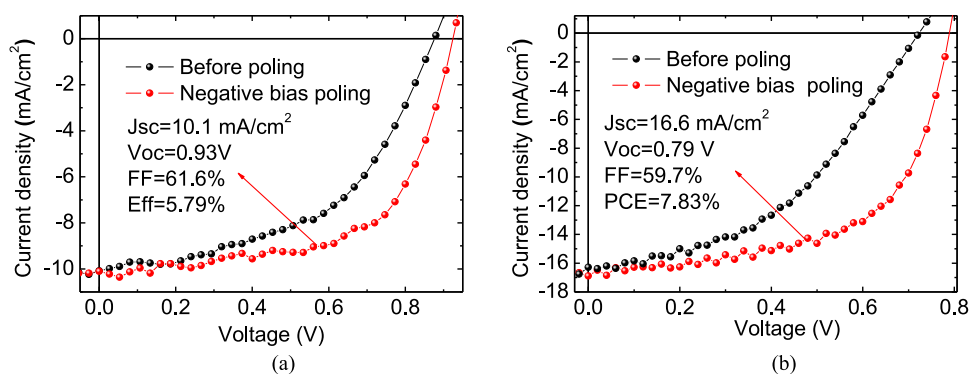
Fig. 6. TPACA polar molecule application in (a) PCDTBT:$PC_{70}BM$ system and (b) PBDTTT-CT:$PC_{70}BM$ system with TPACA blended in the active layer.

After poling, the PCE was significantly increased with enhancements in J_{SC}, V_{OC}, and FF. In addition, negative bias poling of the solar cells based on TPACA blended in P3HT:$PC_{60}BM$ active layer can increase the efficiency, which is consistent with the dark current and capacitance studies. TPACA showed universal applications in enhancing the performance of other low-bandgap polymers. For example, an efficiency of 7.83% was achieved for PBDTTT-CT-based solar cells after poling. This contribution offers a general method to tune the internal electric field to enhance the performance of OSCs and sheds light on understanding the mechanism of the charge generation and extraction in OSCs.

REFERENCES

[1] G. Yu, J. Gao, J. Hummelen, F. Wudl, and A. Heeger, "Polymer photovoltaic cells: enhanced efficiencies via a network of internal donor-acceptor heterojunctions," *Science*, vol. 270, pp. 1789–1790, 1995.

[2] G. Li, R. Zhu, and Y. Yang, "Polymer solar cells," *Nat. Photonics*, vol. 6, pp. 153–161, 2012.

[3] Z. He *et al.*, "Enhanced power-conversion efficiency in polymer solar cells using an inverted device structure," *Nat. Photonics*, vol. 6, pp. 591–595, 2012.

[4] Y. Liu *et al.*, "Aggregation and morphology control enables multiple cases of high-efficiency polymer solar cells," *Nat. Commun.*, vol. 5, pp. 5293, 2014.

[5] C. C. Chen *et al.*, "An efficient triple-junction polymer solar cell having a power conversion efficiency exceeding 11%," *Adv. Mater.*, vol. 26, pp. 5670–5677, 2014.

[6] A. R. Bin Mohd Yusoff *et al.*, "A high efficiency solution processed polymer inverted triple-junction solar cell exhibiting a power conversion efficiency of 11.83%," *Energy Environ. Sci.*, vol. 8, pp. 303–316, 2015.

[7] F. Cheng *et al.*, "Enhancing the performance of P3HT: ICBA based polymer solar cells using LiF as electron collecting buffer layer and UV–ozone treated M_oO_3 as hole collecting buffer layer," *Sol. Energy Mater.*, vol. 110, pp. 63–68, 2013.

[8] H.-H. Liao, L.-M. Chen, Z. Xu, G. Li, and Y. Yang, "Highly efficient inverted polymer solar cell by low temperature annealing of Cs_2CO_3 interlayer," *Appl. Phys. Lett.*, vol. 92, p. 173303, 2008.

[9] M. H. Park, J. H. Li, A. Kumar, G. Li, and Y. Yang, "Doping of the metal oxide nanostructure and its influence in organic electronics," *Adv. Func. Mater.*, vol. 19, pp. 1241–1246, 2009.

[10] S. K. Hau *et al.*, "Air-stable inverted flexible polymer solar cells using zinc oxide nanoparticles as an electron selective layer," *Appl. Phys. Lett.*, vol. 92, p. 253301, 2008.

[11] A. Tada, Y. Geng, Q. Wei, K. Hashimoto, and K. Tajima, "Tailoring organic heterojunction interfaces in bilayer polymer photovoltaic devices," *Nat. Mater.*, vol. 10, pp. 450–455, 2011.

[12] A. Liu *et al.*, "Control of electric field strength and orientation at the donor-acceptor interface in organic solar cells," *Adv. Mater.*, vol. 20, pp. 1065–1070, 2008.

[13] Y. Zhong, J. Ma, K. Hashimoto, and K. Tajima, "Electric field-induced dipole switching at the donor/acceptor interface in organic solar cells," *Adv. Mater.*, vol. 25, pp. 1071–1075, 2013.

[14] L. Chen, C. Xie, and Y. Chen, "Self-assembled conjugated polyelectrolyte-ionic liquid crystal complex as an interlayer for polymer solar cells: Achieving performance enhancement via rapid liquid crystal-induced dipole orientation," *Macromolecules*, vol. 47, pp. 1623–1632, 2014.

[15] Y. Yuan *et al.*, "Efficiency enhancement in organic solar cells with ferroelectric polymers," *Nat. Mater.*, vol. 10, pp. 296–302, 2011.

[16] B. Yang *et al.*, "Tuning the energy level offset between donor and acceptor with ferroelectric dipole layers for increased efficiency in bilayer organic photovoltaic cells," *Adv. Mater.*, vol. 24, pp. 1455–1460, 2012.

[17] Z. Xiao *et al.*, "Synthesis and application of ferroelectric P (VDF-TrFE) nanoparticles in organic photovoltaic devices for high efficiency," *Adv. Energy Mater.*, vol. 3, pp. 1581–1588, 2013.

[18] Y. Yuan *et al.*, "Understanding the effect of ferroelectric polarization on power conversion efficiency of organic photovoltaic devices," *Energy Environ. Sci.*, vol. 5, pp. 8558–8563, 2012.

[19] T. Marinado *et al.*, "How the nature of triphenylamine-polyene dyes in dye-sensitized solar cells affects the open-circuit voltage and electron lifetimes," *Langmuir*, vol. 26, pp. 2592–2598, 2009.

[20] L. Zhou, C. Jia, Z. Wan, X. Chen, and X. Yao, "Effect of imidazole derivatives in triphenylamine-based organic dyes for dye-sensitized solar cells," *Organ. Electron.*, vol. 14, pp. 1755–1762, 2013.

[21] E. Verploegen *et al.*, "Effects of thermal annealing upon the morphology of polymer-fullerene blends," *Adv. Func. Mater.*, vol. 20, pp. 3519–3529, 2010.

[22] K. S. Nalwa *et al.*, "Enhanced charge separation in organic photovoltaic films doped with ferroelectric dipoles," *Energy Environ. Sci.*, vol. 5, pp. 7042–7049, 2012.

[23] W. Liu, Y. Chen, A. Balandin, and K. Wang, "Capacitance-voltage spectroscopy of trapping states in GaN/AlGaN heterostructure field-effect transistors," *J. Nanoelectron. Optoelectron.*, vol. 1, pp. 258–263, 2006.

[24] C. Deibel, T. Strobel, and V. Dyakonov, "Role of the charge transfer state in organic donor-acceptor solar cells," *Adv. Mater.*, vol. 22, pp. 4097–4111, 2010.

[25] T. M. Clarke and J. R. Durrant, "Charge photogeneration in organic solar cells," *Chem. Rev.*, vol. 110, pp. 6736–6767, 2010.

[26] T. Offermans, S. C. Meskers, and R. A. Janssen, "Time delayed collection field experiments on polymer: Fullerene bulk-heterojunction solar cells," *J. Appl. Phys.*, vol. 100, p. 074509, 2006.

[27] J. Kniepert, M. Schubert, J. C. Blakesley, and D. Neher, "Photogeneration and recombination in P3HT/PCBM solar cells probed by time-delayed collection field experiments," *J. Phys. Chem. Lett.*, vol. 2, pp. 700–705, 2011.

[28] B. Yang, Y. Yuan, and J. Huang, "Reduced bimolecular charge recombination loss in thermally annealed bilayer heterojunction photovoltaic devices with large external quantum efficiency and fill factor," *J. Phys. Chem. C*, vol. 118, pp. 5196–5202, 2014.

[29] M. Gluecker, A. Foertig, V. Dyakonov, and C. Deibel, "Impact of nongeminate recombination on the performance of pristine and annealed P3HT: PCBM solar cells," *Phys. Status Solidi (RRL)*, vol. 6, pp. 337–339, 2012.

[30] Z. Xiao *et al.*, "Universal formation of compositionally graded bulk heterojunction for efficiency enhancement in organic photovoltaics," *Adv. Mater.*, vol. 26, pp. 3068–3075, 2014.